Front. Phys. 13(1), 136102 (2018)
https://doi.org/10.1007/s11467-017-0725-3

RESEARCH ARTICLE

Core-softened potentials, multiple liquid–liquid critical points, and density anomaly regions: An exact solution

Eduardo O. Rizzatti[1], **Marco Aurélio A. Barbosa**[2,†], **Marcia C. Barbosa**[1,‡]

[1] *Instituto de Física, Universidade Federal do Rio Grande do Sul, Porto Alegre-RS, Brazil*
[2] *Programa de Pós-Graduacão em Ciência de Materiais, Universidade de Brasília, Planaltina-DF, Brazil*
Corresponding authors. E-mail: [†] *aureliobarbosa@unb.br;* [‡] *marcia.barbosa@ufrgs.br*
Received March 2, 2017; accepted July 27, 2017

The pressure versus temperature phase diagram of a system of particles interacting through a multiscale shoulder-like potential is exactly computed in one dimension. The N-shoulder potential exhibits N density anomaly regions in the phase diagram if the length scales can be connected by a convex curve. The result is analyzed in terms of the convexity of the Gibbs free energy.

Keywords density anomalies regions

PACS numbers 61.20.Gy, 65.20.-w

1 Introduction

The phase behavior of single-component systems considered as particles interacting via the so-called core-softened (CS) potential has received attention since the work of Hemmer and Stell [1]. These potentials exhibit a repulsive core with a softened region having a shoulder or a ramp [1–12]. These models are motivated by the desire to construct a simple two-body isotropic potential capable of describing the complicated features of systems interacting via isotropic potentials. This procedure generates models that are analytically and computationally tractable, and that one hopes are capable of retaining the qualitative features of real complex systems.

The physical motivation behind these studies is the recently acknowledged possibility that some single-component systems exhibit the coexistence of two different liquid phases [1, 2, 6]. This has opened a discussion about the relationship among the presence of two liquid phases, the existence of thermodynamic anomalies in the liquids, and the form of the potential. The case of water has probably been the most intensively studied. For instance, liquid water has a temperature at which the density is maximum at constant pressure [13]. It was proposed some time ago that the temperature of maximum density (TMD) might be associated with a critical point at the terminus of a liquid–liquid phase transition [14]. This hypothesis has been supported by simulations [14, 15] and experiments [16, 17].

The natural question that follows is whether a CS potential with two length scales will have one region in the pressure versus temperature phase diagram in which the density is anomalous and a liquid–liquid phase transition is present, and one with three length scales will have two TMD lines. To address this question, in this paper, we present an exact solution of a system of particles interacting through a multi-length-scale potential. Our analysis, even though it is restricted to one dimension, shows that the TMD lines are associated with the presence of liquid–liquid critical points. The existence of both various TMD lines and critical points depends on the shape of the pair interaction potential. If the length scales can be connected by a convex curve, multiple TMDs are present; otherwise, they are absent.

The rest of the paper is structured as follows. In Section 2, the exact solution is presented and applied to the one-shoulder, two-shoulder, and multiple-shoulder potentials. In Section 3, the analytic solution is applied to the lattice version of the model. Conclusions are presented in Section 4.

*Special Topic: Water and Water Systems (Eds. F. Mallamace, R. Car, and Limei Xu).

2 Analytic solution

We consider a one-dimensional system composed of a set of identical classical particles of mass m that interact only with their nearest neighbors. As the problem is treated using classical mechanics, we can assign to the particles moving on this line the positions $\boldsymbol{q} = (q_1, \ldots, q_N)$ and linear momenta $\boldsymbol{p} = (p_1, \ldots, p_N)$. The time evolution is described by the Hamiltonian

$$\mathscr{H}(\boldsymbol{q}, \boldsymbol{p}) = \frac{\boldsymbol{p}^2}{2m} + U(\boldsymbol{q}), \tag{1}$$

where U is the total potential energy. In addition, we suppose that interaction occurs among adjacent pairs through a potential Φ that is translationally invariant; U is then expressed as

$$U(\boldsymbol{q}) = \sum_{i=1}^{N-1} \Phi(q_{i+1} - q_i), \tag{2}$$

where $\Phi(q_{i+1} - q_i)$ is the potential energy between two particles.

The pressure ensemble corresponds to a system in thermodynamic equilibrium with heat and volume reservoirs, which fix the temperature $\beta^{-1} = k_B T$ and pressure p. A simplified expression for the partition function J is given by [18, 19]

$$J(T, p, N) = \frac{1}{(\beta p)^2 \Lambda_0 \Lambda^N} \left(\int_0^\infty \mathrm{e}^{-\beta[\Phi(r)+pr]} \mathrm{d}r \right)^{N-1}, \tag{3}$$

where $\beta = 1/(k_B T)$, Λ_0 is a constant with dimensions of length, and Λ is the de Broglie thermal wavelength, namely,

$$\Lambda(T) = \left(\frac{h^2}{2\pi m k_B T} \right)^{1/2}. \tag{4}$$

In the thermodynamic limit, where $N \to \infty$, the Gibbs free energy per particle is then expressed as

$$\begin{aligned} g(T, p) &= -k_B T \lim_{N\to\infty} \frac{1}{N} \log J \\ &= -\frac{1}{\beta} \log \frac{1}{\Lambda} \left(\int_0^\infty \mathrm{e}^{-\beta[\Phi(r)+pr]} \mathrm{d}r \right). \end{aligned} \tag{5}$$

From this fundamental equation follows the equation of state,

$$\begin{aligned} v(T, p) &= \frac{\partial g(T, p)}{\partial p}, \\ \rho(T, p) &= \frac{1}{v(T, p)}, \end{aligned} \tag{6}$$

allowing us to map the behavior of the isobaric thermal expansion coefficient given by

$$\alpha(T, p) = \frac{1}{v} \left(\frac{\partial v}{\partial T} \right)_p. \tag{7}$$

3 Continuous potentials

3.1 One-shoulder pair potential

We begin by analyzing the simplest two-length scale potential Φ:

$$\Phi(r) = \begin{cases} \infty, & r < \lambda_0 \\ V_0, & \lambda_0 \le r < \lambda_1 \\ V_1, & \lambda_1 \le r. \end{cases} \tag{8}$$

Figure 1(a) shows the interparticle potential energy, $\Phi^* = \Phi/V_0$, versus the distance between particles, $r^* = r/\lambda_0$, where $V_1 = 0$, $\lambda_0 < \lambda_1 < 2\lambda_0$, and $\lambda_1^* = \lambda_1/\lambda_0$. For these reduced units, the Gibbs free energy in Eq. (5)

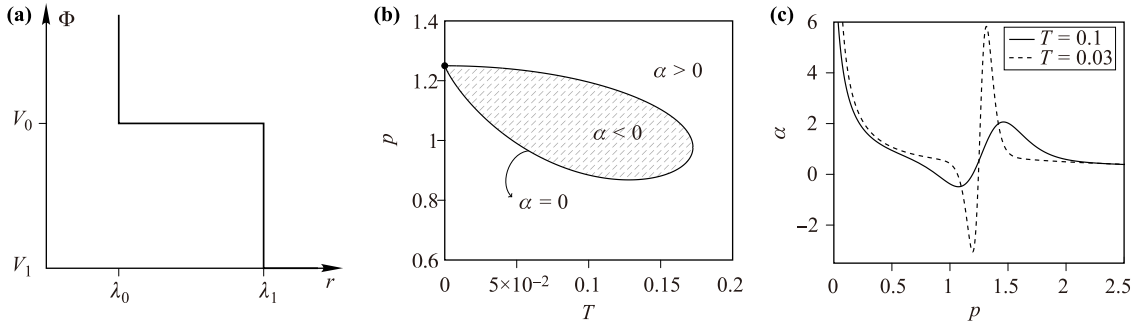

Fig. 1 **(a)** Pair potential $\Phi^* = \Phi/V_0$ versus $r^* = r/\lambda_0$, **(b)** pressure versus temperature, and **(c)** thermal expansion coefficient versus pressure for $\lambda_1^* = \lambda_1/\lambda_0$.

assumes the form

$$g^*(T,p) \equiv \frac{g(T,p)}{V_0} = -T^* \log \frac{T^*}{\Lambda^* p^*}\left[e^{-(1+p^*)/T^*} - e^{-(1+\lambda_1^* p^*)/T^*} + e^{-(V_1^*+\lambda_1^* p^*)}\right], \quad (9)$$

where the temperature, pressure, and thermal wavelength in reduced units are given by $T^* = k_B T/V_0$, $p^* = p\lambda_0/V_0$, and $\Lambda^* = \Lambda/\lambda_0$, respectively, and the potential parameters are $\lambda_1^* = \lambda_1/\lambda_0$ and $V_1^* = V_1/V_0$.

The density versus temperature plot for a fixed pressure reveals the temperature at which the density is maximum. For different pressures, this maximum occurs at different temperatures, as illustrated in Fig. 1(b). The intuitive idea behind this is that competition between the two length scales in the potential generates a density maximum if both scales are accessible to the system [20–24]. The anomaly then manifests itself when the system passes from a less dense structure associated with the scale λ_1 to a more compact one associated with λ_0 when the temperature is increased at a fixed pressure. Furthermore, the response function α, shown in Fig. 1(c), not only changes sign, indicating the presence of a density anomaly region in the pressure versus temperature phase diagram, but also diverges as $T \to 0$, a behavior that is generally related to the presence of criticality [23].

One-dimensional systems with finite-range interactions, such as the model we are analyzing, obviously exhibit phase transitions only at $T = 0$. The temperature destroys any attempt at ordering. Indeed, Takahashi's solution [18], which is illustrated in Eq. (3), does not violate this principle.

Let us analyze, therefore, the zero-temperature phase transitions in order to establish a relationship with the density anomaly regions. First, let us fix $p > 0$. The leading behavior of $g(T,p)$ depends essentially on the argument of its exponentials in Eq. (9). In this case, the condition $\lambda_1 > \lambda_0$ implies $V_0 + \lambda_0 p < V_0 + \lambda_1 p$ for every $p > 0$; consequently,

$$\lim_{\beta\to\infty} g = -\lim_{\beta\to\infty} \frac{1}{\beta} \log\left[e^{-\beta(V_0+\lambda_0 p)} + e^{-\beta(V_1+\lambda_1 p)}\right]. \quad (10)$$

Hence, this limit is determined by the straight lines $\eta_0(p) = V_0 + \lambda_0 p$ and $\eta_1(p) = V_1 + \lambda_1 p$ of smallest value at a particular pressure p, as shown in Fig. 2(a). By defining their intersection as

$$p_{01} = \frac{V_0 - V_1}{\lambda_1 - \lambda_0}, \quad (11)$$

we can express $g = g(p)$ in this regime, as illustrated in Fig. 2(a), as

$$g(p) = \begin{cases} -\infty, & p = 0 \\ V_1 + \lambda_1 p, & 0 < p < p_{01} \\ V_0 + \lambda_0 p, & p_{01} < p. \end{cases} \quad (12)$$

In the ground state, $g(p)$, despite its well-defined concavity, as a function of p exhibits singularities at the origin ($p = 0$) and at $p = p_{01}$. At $p = p_{01}$, the system undergoes a discontinuous phase transition in which the high-density phase, $v = \lambda_0$, associated with the length scale λ_0 coexists with the low-density phase, $v = \lambda_1$, associated with λ_1, according to Fig. 2(b). This suggests a mechanism for the density anomaly. Its origin should be related to the phase separation at $T = 0$. The system at zero temperature and p_{01} has two coexisting phases. As the temperature increases, the competition between these two phases give rise to the density anomaly.

We can extend this analysis and look for a connection between the interaction potential Φ and the thermodynamic anomaly. This can be approached through the expected value $\langle\Phi\rangle$, which is defined for equilibrium states as the probability measure of the pressure ensemble and expressed as

$$\langle\Phi\rangle = u - \frac{1}{2}k_B T. \quad (13)$$

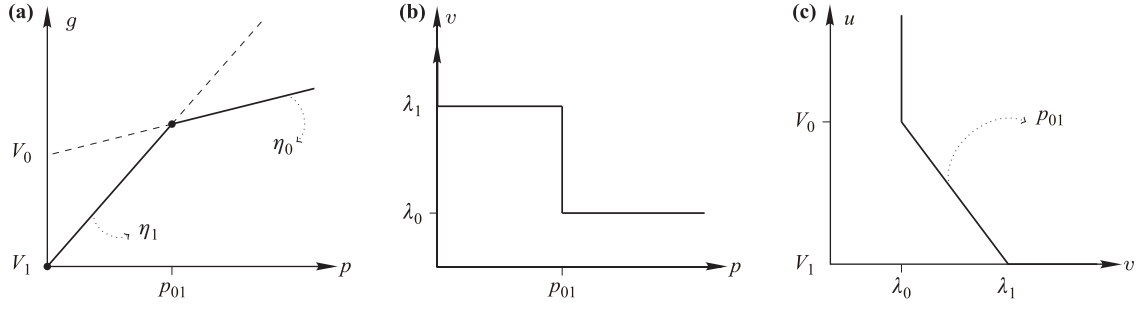

Fig. 2 **(a)** Gibbs free energy g as a function of the pressure p for $T = 0$ (solid line; the singularity at $p = 0$ was omitted); the coexistence pressure p_{01} is just the intersection of η_0 and η_1. **(b)** Specific volume v versus p follows from the slopes of these lines. **(c)** Internal energy representation of the same system.

Hence, for $T \to 0$, the expected value of the potential coincides with the internal energy of the system. This result allows us to employ the internal energy representation $u = u(v)$ instead of the Gibbs representation. By performing the Legendre transformation[1)] between the conjugate variables $(v, -p)$, we obtain the energy

$$u(v) = \sup_p \{g(p) - pv\}. \tag{14}$$

Figure 2(c) shows the energy versus the pressure; as expected, the internal energy is a convex function of its argument, whereas its magnitude is the slope of the coexistence pressure p_{01}.

3.2 Two-shoulder pair potential

Next, we explore the possibility that there are two regions in the pressure versus temperature phase diagram where a density anomaly and criticality appear as the system interacts through a potential with three length scales. When another scale of interaction is added, the interaction potential Φ is given by

$$\Phi(r) = \begin{cases} \infty, & r < \lambda_0 \\ V_0, & \lambda_0 \le r < \lambda_1 \\ V_1, & \lambda_1 \le r < \lambda_2 \\ V_2, & \lambda_2 \le r, \end{cases} \tag{15}$$

where $V_2 = 0$, and $\lambda_0 < \lambda_1 < \lambda_2 < 2\lambda_0$, as shown in Fig. 3.

Then, the Gibbs fundamental equation [Eq. (5)] of this system is expressed as

$$g(\beta, p) = -\frac{1}{\beta} \log \frac{1}{\Lambda \beta p} \Big[e^{-\beta(V_0+\lambda_0 p)} - e^{-\beta(V_0+\lambda_1 p)} + e^{-\beta(V_1+\lambda_1 p)} - e^{-\beta(V_1+\lambda_2 p)} + e^{-\beta(V_2+\lambda_2 p)} \Big]. \tag{16}$$

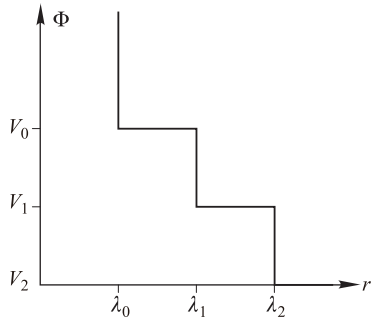

Fig. 3 Pair potential versus distance with three length scales.

[1)] It is well defined because $\lim_{T\to 0} Ts(T,p) = 0$, where $s = s(T,p)$ is the entropy per particle.

It is reasonable to expect that the inclusion of a new scale of interaction allows for the occurrence of a new density anomaly region in the phase diagram. However, Fig. 4 shows that, depending on the choice of parameters, the system exhibits just one or two density anomaly regions in the pressure versus temperature phase diagram. The origin of this behavior can be understood if we analyze the ground-state phase transitions, which are precursors of density anomalies, as seen in the former section. First, take $p > 0$; then the zero-temperature Gibbs free energy is given by

$$\lim_{\beta\to\infty} g = -\lim_{\beta\to\infty} \frac{1}{\beta} \log \Big[e^{-\beta(V_0+\lambda_0 p)} + e^{-\beta(V_1+\lambda_1 p)} + e^{-\beta(V_2+\lambda_2 p)} \Big]. \tag{17}$$

The zero-temperature Gibbs free energy is determined by the smallest value among the straight lines $\eta_0(p) = V_0 + \lambda_0 p$, $\eta_1(p) = V_1 + \lambda_1 p$, and $\eta_2(p) = V_2 + \lambda_2 p$ for a particular pressure p. If we define their intersections as

$$p_{01} = \frac{V_0 - V_1}{\lambda_1 - \lambda_0}, \quad p_{02} = \frac{V_0 - V_2}{\lambda_2 - \lambda_0},$$

and

$$p_{12} = \frac{V_1 - V_2}{\lambda_2 - \lambda_1}, \tag{18}$$

two possible scenarios arise: $p_{01} \le p_{12}$ or $p_{01} > p_{12}$ (a consequence of the restrictions $\lambda_0 < \lambda_1 < \lambda_2$). It follows that $g = g(p)$ in this regime [see Figure 5(a) and 5(b)] assumes the form

$$g(p) = \begin{cases} -\infty, & p = 0 \\ V_2 + \lambda_2 p, & 0 < p < p_{02} \\ V_0 + \lambda_0 p, & p_{02} < p \end{cases} \tag{19}$$

if $p_{01} \le p_{12}$, or the form

$$g(p) = \begin{cases} -\infty, & p = 0 \\ V_2 + \lambda_2 p, & 0 < p < p_{12} \\ V_1 + \lambda_1 p, & p_{12} < p < p_{01} \\ V_0 + \lambda_0 p, & p_{01} < p \end{cases} \tag{20}$$

if $p_{01} > p_{12}$. Therefore, the phase diagram shows only one density anomaly region in the pressure versus temperature phase diagram in the first case and two density anomaly regions in the second case.

To visualize the energetic conditions for the existence of one or two density anomaly regions in the pressure versus temperature phase diagram, the behavior of Φ at $T = 0$ is analyzed. Eq. (13) shows that at $T = 0$, $\Phi = u(v)$. Therefore, in Fig. 4(a), the slopes of the lines joining the points (λ_0, V_0), (λ_1, V_1), and (λ_2, V_2) are equal in magnitude to the coexistence pressures defined by Eq. (18). The condition $p_{01} > p_{12}$, illustrated

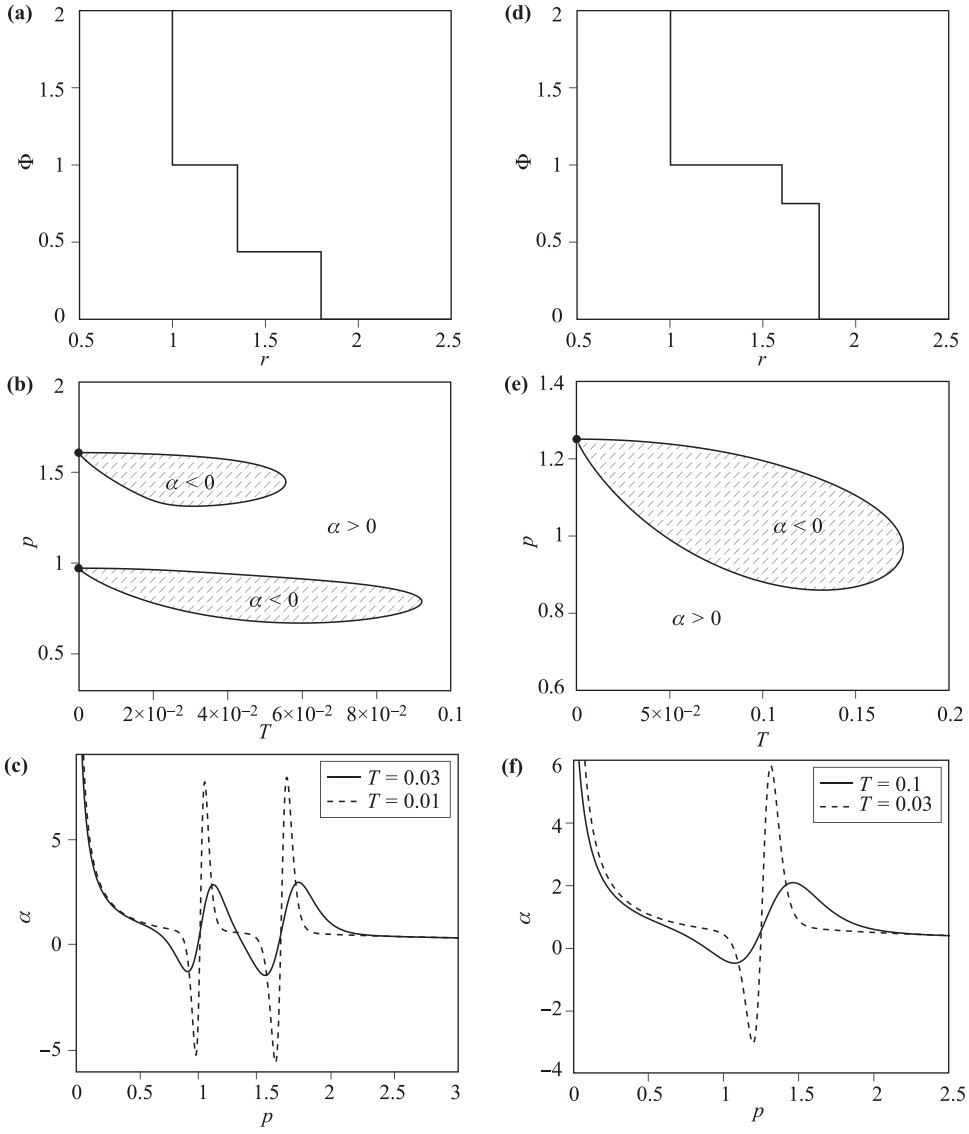

Fig. 4 Potential Φ versus r for $\lambda_2 = 1.8$, $\lambda_1 = 27/20$, $\lambda_0 = 1$, $V_1 = 7/16$, and and $V_0 = 1$ **(a)** and $\lambda_2 = 1.8$, $\lambda_1 = 1.6$, $\lambda_0 = 1$, $V_1 = 0.75$, and $V_0 = 1$ **(d)**. The corresponding phase diagrams exhibiting the density anomaly states are shown in **(b)** and **(e)**, respectively. The divergence of the response function α at the critical pressures as the system approaches $T = 0$, as well as its sign change, are shown in **(c)** and **(f)**, respectively.

in Fig. 4(b), permits all scales to be accessible inasmuch as it generates a convex u (phases of lower volume coexist at a pressure higher than phases of higher volume; translating this idea to our notation, stability requires $p_{01} > p_{12}$ for $\lambda_0 < \lambda_1 < \lambda_2$). Thus, the transitions 01 and 12 are allowed. Consequently, the thermal expansion coefficient shown in Fig. 4(c) exhibits two regions with divergence as $T \to 0$. On the other hand, if Φ versus distance behaves as shown in Fig. 4(d), $p_{01} \leq p_{12}$. The length scale, (λ_1, V_1), becomes inaccessible because its location implies a nonconvex u as a function of the specific volume. The system then coexists only in phases 0 and 2, as illustrated in Fig. 4(e). In this case, the divergence of the thermal expansion coefficient is similar to that in the system with two length scales, as shown in Fig. 4(f).

We can easily identify, for $T = 0$, whether the system has one or two density anomaly regions in the pressure versus temperature phase diagram by using the following geometric picture. First, we draw one straight line connecting (λ_0, V_0) and (λ_1, V_1) and another straight line connecting (λ_1, V_1) and (λ_2, V_2) in the potentials illustrated in Figs. 5(a) and (e). In Fig. 5(a), the two lines together form a convex curve, and two density anomaly regions are present, whereas in Fig. 5(e), a concave curve is present, and just one density anomaly region is present.

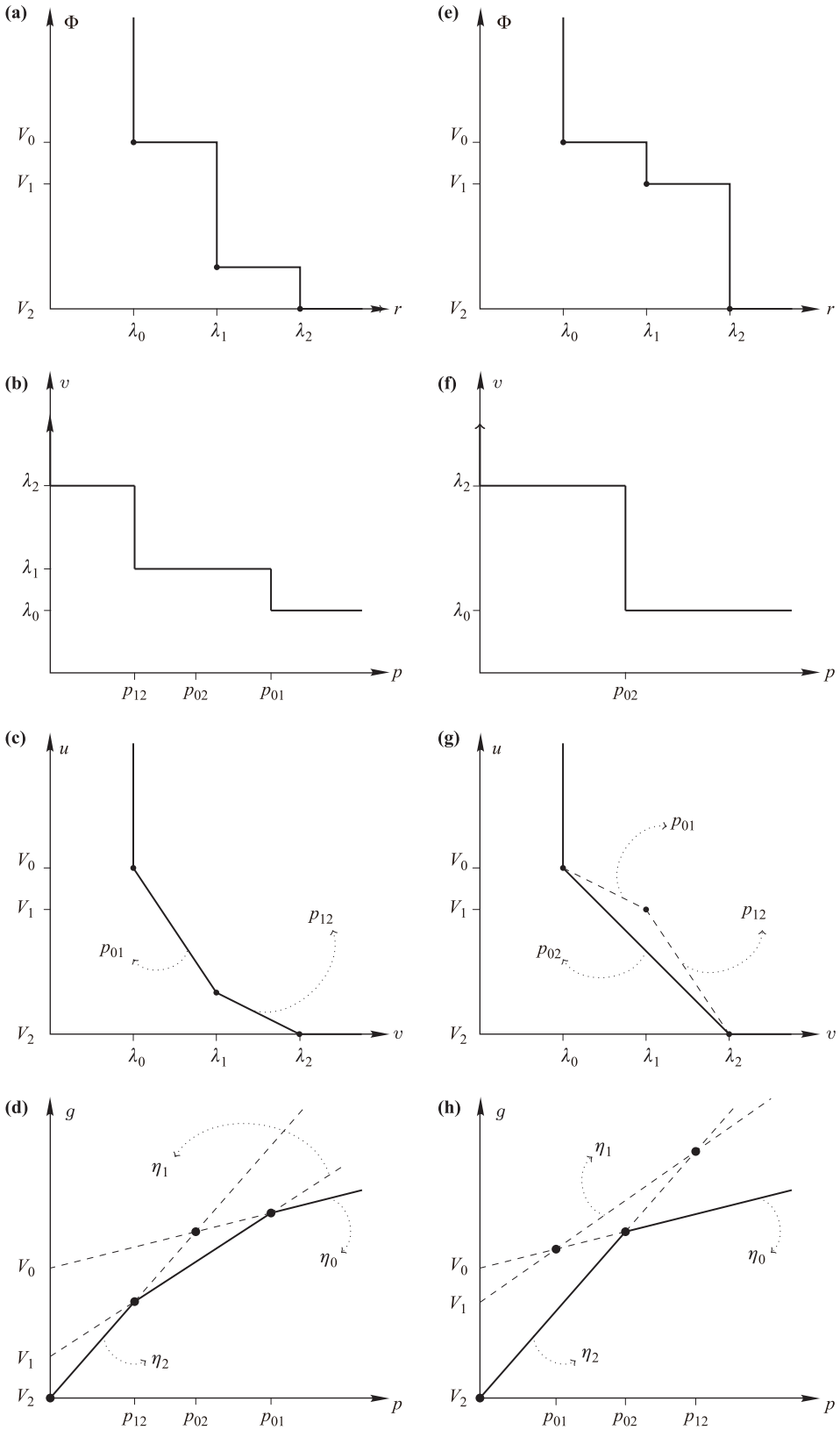

Fig. 5 Φ versus r for **(a)** $p_{01} \leq p_{12}$ and **(e)** $p_{01} > p_{12}$; v versus p for **(b)** $p_{01} \leq p_{12}$ and **(f)** $p_{01} > p_{12}$; u versus v for **(c)** $p_{01} \leq p_{12}$ and **(g)** $p_{01} > p_{12}$; and g versus p for **(d)** $p_{01} \leq p_{12}$ and **(h)** $p_{01} > p_{12}$.

The difference in the two cases is also reflected in the reduced volume versus pressure diagram, which shows three phases in Fig. 5(b) and two phases in Fig. 5(f). Consequently, the internal energy u versus v shows three stable densities in Fig. 5(c) and only two in Fig. 5(g). Finally, the free energy g as a function of p is a concave stable function with three densities in Fig. 5(d) and only two in Fig. 5(h).

Another way to visualize whether a pair potential leads to multiple density anomaly regions is to draw a line connecting (λ_0, V_0) and (λ_1, V_1), another straight line connecting (λ_1, V_1) and (λ_2, V_2), and a third line connecting (λ_0, V_0) and (λ_2, V_2). If the first two lines lie above the third line, the system has two density anomaly regions.

This same argument will be generalized in the following section, where we will deal with the limit of N shoulders.

3.3 Infinite-shoulder pair potential

In this section, let us consider an extrapolation of the interaction potential Φ of the form

$$\Phi(r) = \begin{cases} \infty, & r < \lambda_0 \\ V_0, & \lambda_0 \le r < \lambda_1 \\ \vdots & \\ V_i, & \lambda_i \le r < \lambda_{i+1} \\ \vdots & \\ V_N, & \lambda_N \le r < \lambda_{N+1}, \end{cases} \tag{21}$$

where $V_N = 0$, $\lambda_0 < \ldots < \lambda_i < \ldots < \lambda_N < 2\lambda_0$, and $\lambda_{N+1} \to \infty$. The Gibbs free energy g associated with this potential is

$$g(\beta, p) = -\frac{1}{\beta} \log \left[\frac{1}{\Lambda \beta p} \times \sum_{i=0}^{N} \left(\mathrm{e}^{-\beta(V_i + \lambda_i p)} - \mathrm{e}^{-\beta(V_i + \lambda_{i+1} p)} \right) \right]. \tag{22}$$

In the ground state, the free energy behaves as

$$\lim_{\beta \to \infty} g = -\lim_{\beta \to \infty} \frac{1}{\beta} \log \left[\sum_{i=0}^{N} \mathrm{e}^{-\beta(V_i + \lambda_i p)} \right] \tag{23}$$

for $\lambda_i < \lambda_{i+1}$ and $0 \le i \le N$. If we define the straight lines

$$\eta_i(p) = V_i + \lambda_i p \tag{24}$$

for $0 \le i \le N$, the ground-state free energy becomes

$$g(p) = \inf_{0 \le i \le N} \eta_i(p) \tag{25}$$

for $p > 0$. The intersection of the $\eta_i(p)$ and $\eta_j(p)$ lines represents the possible coexistence pressures between phases i and j:

$$p_{ij} = \frac{V_i - V_j}{\lambda_j - \lambda_i}, \tag{26}$$

where $0 \le i < j \le N$.

For this multiscale system, the fundamental question is whether a scale (λ_k, V_k) determines a phase transition and consequently a density anomaly region. In other words, if there exists an interval I_k (on the domain of g) such that $p \in I_k$, this implies that $g(p) = V_k + \lambda_k p$. This happens only if $p_{ik} > p_{kj}$ for all i, j obeying $i < k < j$ (i.e., $\lambda_i < \lambda_k < \lambda_j$); $N+1$ phases and N density anomaly regions are present in the system.

Figure 6(a) shows the free energy versus pressure for a system with $N+1$ phases and N density anomaly regions, whereas Fig. 6(c) shows the free energy versus pressure for a system with N phases and $N-1$ density anomaly regions. The internal energies of these two systems are shown in Figs. 6(b) and (d), respectively.

4 Lattice pair potentials

The previous section presented an analysis of one-dimensional systems interacting through shoulder pair potentials in continuous space. We found that the existence of many density anomaly regions in the pressure versus temperature phase diagram depends on the convexity of Φ. In this section, we test the generality of this result regarding the convexity of Φ for a lattice system. We consider a lattice gas model with a four-shoulder pair potential that is restricted to a lattice whose sites are regularly spaced by $l = l_0$, with $l_0 = 1$ (reduced units). A partition function similar to that derived in the previous section [Eq. (3)] but for a lattice system is given by $J(\beta, p, N)$:

$$J(\beta, p, N) = \left[\sum_r \mathrm{e}^{-\beta \eta_r(p)} \right]^N, \tag{27}$$

where $\eta_r(p)$ was defined above.[2)] It follows that an exact expression for g is simply

$$g = -\frac{1}{\beta} \ln \left[\sum_{r=1}^{\infty} \mathrm{e}^{-\beta \eta_r(p)} \right], \tag{28}$$

which is identical to the low-temperature limit obtained for continuous models in Eq. (23). Thus, the restrictions obtained above for the scales (λ_k, u_k) on the continuous model can be applied to lattice models.

[2)] Note that $\eta_r(p)$ was previously interpreted as the microscopic enthalpy for a pair of successive particles in previous works, with $\eta_r(p) = h(r; p)$ [23, 25].

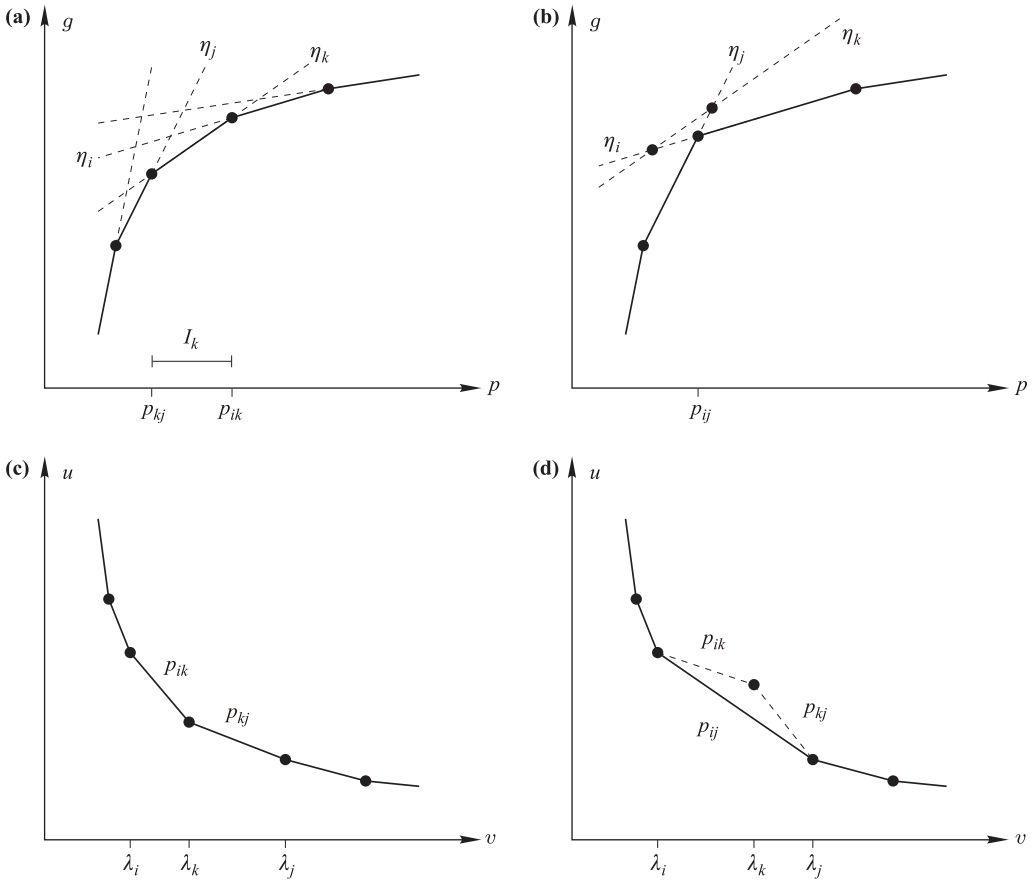

Fig. 6 Ground-state potentials $g = g(p)$ and $u = u(v)$ for the two scenarios described here.

As an application, we design a simple lattice gas model pair potential presenting five states in the ground state and four phase transitions between fluid phases.[3)] The critical pressures are set to $p_{k,k+1} = 5 - k$, where the molecules in phase k are separated by k lattice sites. With this definition, the critical pressures are simply $\{p_{4,5} = 1, p_{3,4} = 2, p_{2,3} = 3, p_{1,2} = 4\}$, and a pair potential with this behavior can be found by starting with $u_5 = 0$ and recursively calculating u_k from Eq. (26). The resulting pair potential is shown in Fig. 7.

The pressure versus temperature phase diagram of the model is shown in Fig. 7, where ground-state phase transitions between different fluids are indicated by filled circles, at the expected pressures $p = 1, 2, 3, 4$, and a gas–liquid transition is indicated by a filled triangle at $p = 0$.

The TMD line is also shown in the upper right panel of Fig. 7. The TMD line emanates from each ground-state phase transition, creating four regions of negative thermal expansion coefficient, i.e., regions where the density anomalously increases with temperature at fixed pressure. Each TMD line reaches a maximum temperature and returns to a lower temperature, reaching the ground state at a pressure that is exactly between two critical points. The exact location for the endpoints of these TMD lines can be explained by the competing effects of contraction and expansion on the stable ground-state configuration (a similar calculation was described in Ref. [25]).

We finish discussing this example by investigating the behavior of thermal expansion as a function of pressure at fixed temperature. In the last panel of Fig. 7, α oscillates when crossing pressures near the critical value, indicating a relationship between phase transitions and density anomalies in one-dimensional systems. This result is consistent and was also found in other one-dimensional lattice models [24, 25], three-dimensional CS fluids [23], and the continuous one-dimensional systems investigated here.

5 Conclusions

In this paper, we obtained an exact solution for a family of one-dimensional potentials that are characterized by having N shoulders. The presence of one shoulder re-

[3)] For simplicity, neither the gas phase nor the liquid–gas phase transition are numbered.

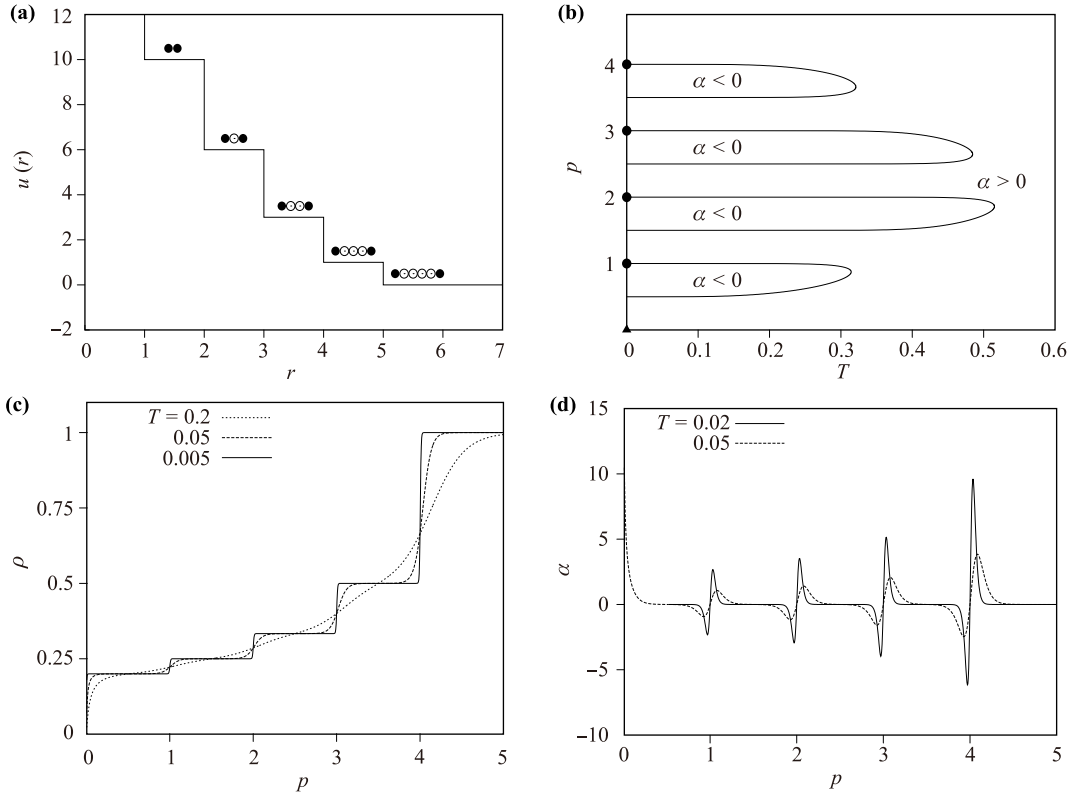

Fig. 7 **(a)** Pair potential exhibiting different phases, **(b)** pressure versus temperature phase diagram illustrating the TMD line, **(c)** density versus pressure for different temperatures, and **(d)** thermal expansion coefficient versus pressure for different temperatures.

sults in a density anomaly region in the pressure versus temperature phase diagram, and consequently, a zero-temperature liquid–liquid phase transition. The presence of two, three, ..., N density anomaly regions for two, three, ..., N shoulders occurs only if the pair potential forms a convex curve when the different length scales are connected.

The prediction in one dimension can be extrapolated to the three-dimensional case, and that for two shoulders results in the existence of two density anomaly regions and two liquid–liquid phase transitions [23].

References

1. P. C. Hemmer and G. Stell, Fluids with Several Phase Transitions, *Phys. Rev. Lett.* 24(23), 1284 (1970)
2. P. G. Debenedetti, V. S. Raghavan, and S. S. Borick, Spinodal curve of some supercooled liquids, *J. Chem. Phys.* 95(11), 4540 (1991)
3. S. Sastry, P. G. Debenedetti, F. Sciortino, and H. E. Stanley, Singularity-free interpretation of the thermodynamics of supercooled water, *Phys. Rev. E* 53(6), 6144 (1996)
4. C. J. Roberts and P. G. Debenedetti, Polyamorphism and density anomalies in network-forming fluids: Zeroth- and first-order approximations, *J. Chem. Phys.* 105(2), 658 (1996)
5. E. A. Jagla, Phase behavior of a system of particles with core collapse, *Phys. Rev. E* 58(2), 1478 (1998)
6. G. Franzese, G. Malescio, A. Skibinsky, S. V. Buldyrev, and H. E. Stanley, Generic mechanism for generating a liquid–liquid phase transition, *Nature* 409(6821), 692 (2001)
7. N. B. Wilding and J. E. Magee, Phase behavior and thermodynamic anomalies of core-softened fluids, *Phys. Rev. E* 66(3), 031509 (2002)
8. P. Camp, Structure and phase behavior of a two-dimensional system with core-softened and long-range repulsive interactions, *Phys. Rev. E* 68(6), 061506 (2003)
9. M. Pretti and C. Buzano, Thermodynamic anomalies in a lattice model of water, *J. Chem. Phys.* 121(23), 11856 (2004)
10. A. Balladares and M. C. Barbosa, Density anomaly in core-softened lattice gas, *J. Phys.: Condens. Matter* 16(49), 8811 (2004)

11. A. B. Oliveira and M. C. Barbosa, Density anomaly in a competing interactions lattice gas model, *J. Phys.: Condens. Matter* 17(3), 399 (2005)
12. Yu. D. Fomin, E. N. Tsiok, and V. N. Ryzhov, Complex phase behavior of the system of particles with smooth potential with repulsive shoulder and attractive well, *J. Chem. Phys.* 134(4), 044523 (2011)
13. G. S. Kell, Precise representation of volume properties of water at one atmosphere, *J. Chem. Eng. Data* 12(1), 66 (1967)
14. P. H. Poole, F. Sciortino, U. Essmann, and H. E. Stanley, Phase behaviour of metastable water, *Nature* 360(6402), 324 (1992)
15. J. C. Palmer, F. Martelli, Y. Liu, R. Car, A. Z. Panagiotopoulos, and P. G. Debenedetti, Metastable liquid–liquid transition in a molecular model of water, *Nature* 510(7505), 385 (2014)
16. A. Faraone, L. Liu, C. Y. Mou, C. W. Yen, and S. H. Chen, Fragile-to-strong liquid transition in deeply supercooled confined water, *J. Chem. Phys.* 121(22), 10843 (2004)
17. J. A. Sellberg, C. Huang, T. A. McQueen, N. D. Loh, H. Laksmono, et al., Ultrafast X-ray probing of water structure below the homogeneous ice nucleation temperature, *Nature* 510, 381 (2014)
18. H. Takahashi, Mathematical Physics in One Dimension, Academic Press, 1966, pp 25–34
19. G. Gallavotti, Statistical Mechanics: A Short Treatise, Berlin: Springer, 1999, pp 162–164
20. A. Barros de Oliveira, P. A. Netz, T. Colla, and M. C. Barbosa, Thermodynamic and dynamic anomalies for a three-dimensional isotropic core-softened potential, *J. Chem. Phys.* 124(8), 084505 (2006)
21. A. Barros de Oliveira, P. A. Netz, T. Colla, and M. C. Barbosa, Thermodynamic and dynamic anomalies for a three-dimensional isotropic core-softened potential, *J. Chem. Phys.* 124(8), 084505 (2006)
22. E. Barraz, Salcedo, and M. C. Barbosa, Thermodynamic, dynamic, and structural anomalies for shoulder-like potentials, *J. Chem. Phys.* 131(9), 094504 (2009)
23. M. A. A. Barbosa, E. Salcedo, and M. C. Barbosa, Multiple liquid-liquid critical points and density anomaly in core-softened potentials, *Phys. Rev. E* 87(3), 032303 (2013)
24. M. A. A. Barbosa, F. V. Barbosa, and F. A. Oliveira, Thermodynamic and dynamic anomalies in a one-dimensional lattice model of liquid water, *J. Chem. Phys.* 134(2), 024511 (2011)
25. F. B. V. da Silva, F. A. Oliveira, and M. A. A. Barbosa, Residual entropy and waterlike anomalies in the repulsive one dimensional lattice gas, *J. Chem. Phys.* 142(14), 144506 (2015)